Journal of Dentistry 121 (2022) 104122

Contents lists available at ScienceDirect

Journal of Dentistry

journal homepage: www.elsevier.com/locate/jdent

Influence of the implant scan body bevel location, implant angulation and position on intraoral scanning accuracy: An *in vitro* study

Miguel Gómez-Polo [a], Francisco Álvarez [a], Rocío Ortega [b], Cristina Gómez-Polo [c], Abdul B. Barmak [d], John C. Kois [e,f,g], Marta Revilla-León [f,h,i,*]

[a] Department of Conservative Dentistry and Prosthodontics, School of Dentistry, Complutense University of Madrid, Madrid, Spain
[b] Department of Prosthetic Dentistry, School of Dentistry, European University of Madrid, Madrid, Spain
[c] Department of Dentistry, School of Medicine, University of Salamanca, Salamanca, Spain
[d] Clinical Research and Biostatistics, Eastman Institute of Oral Health, University of Rochester Medical Center, Rochester, NY, United States
[e] Founder and Director Kois Center, Seattle, WA, United States
[f] Department of Restorative Dentistry, School of Dentistry, University of Washington, 1001 Fairview Ave N # 2200, Seattle, WA 98109, United States
[g] Private Practice, Seattle, WA, United States
[h] Kois Center, Seattle, WA, United States
[i] Researcher at Revilla Research Center, Madrid, Spain

ARTICLE INFO

Keywords:
Accuracy
Digital impression
Implant dentistry
Intraoral scanner
Prosthodontics

ABSTRACT

Purpose: To assess the influence of the scan body geometry bevel location and implant angulation and position of complete-arch implant digital scans.
Material and methods: Two definitive casts with 4 implant analogs placed parallel (*P* group) or angulated up to 30° (NP group) were fabricated. Five subgroups were created based on the scan body geometry bevel position: facial, mesial, distal, lingual, or random (F, M, D, L, and R subgroup). Casts were digitized using a laboratory scanner (reference) (7Series Desktop Scanner) and an intraoral scanner (TRIOS 3). The implant position discrepancies between the reference and experimental scans were calculated. Data was analyzed using 3-way ANOVA and Tukey tests ($\alpha = .05$).
Results: The scan body geometry bevel position ($P < .001$) and the inter-implant distance ($P < .001$) were shown as significant predictors of the linear discrepancies obtained. The L subgroup had a significantly lower discrepancy compared with the other subgroups. Implant angulation ($P < .001$), the scan body geometry bevel position ($P < .001$), and the inter-implant distance ($P < .001$) were all significant predictors on the angular discrepancies obtained.
Conclusions: The scan body geometry bevel location and implant angulation and position influenced the accuracy of the IOS tested. The lingual orientation obtained significantly better accuracy values compared with the other positions. The parallel implant analog position obtained better accuracy than the angulated positions. Lastly, the implant positioned in the dental arch where the intraoral digital scan was finished obtained significantly higher distortion than the contralateral implant.

Clinical significance

To maximize the scanning accuracy (trueness and precision) of complete-arch intraoral digital scans by using the intraoral scanner tested, the implant scan body geometry bevel feature should be positioned with a lingual orientation.

1. Introduction

Intraoral digitization has now become commonly and successfully integrated within clinical dental procedures [1–5]. However, different variables that can affect and decrease intraoral scanning accuracy have been identified such as scanning pattern [6,7], ambient lighting [8–10], technology [11–13], size of the scanner head [14], extension of the digital scan [15,16], operator experience [17–19], characteristics of the

* Corresponding author at: Kois Center.
E-mail address: marta.revilla.leon@gmail.com (M. Revilla-León).

https://doi.org/10.1016/j.jdent.2022.104122
Received 8 November 2021; Received in revised form 31 March 2022; Accepted 3 April 2022
Available online 6 April 2022

surface scanned [20–23], presence of edentulous areas [24], and post-processing procedures [15,25]. Furthermore, for intraoral implant digital scans additional elements might need to be considered including implant scan body selected [26–29], implant angulation [30–33], implant depth [34–36], and inter-implant distance [35–37].

Implant scan bodies assist on the digital transfer of the 3-dimensional position of dental implants from the patient's mouth to computer-aided design (CAD) programs [38]. The geometric design of the implant scan bodies includes a feature that aims to translate the anti-rotational element of the dental implant [39]. However, there is no agreement on the optimal implant scan body material and design [26–29]. Additionally, a geometry bevel feature design on the implant scan body is generally incorporated as flat surfaces over a generally cylindrical body [39]. However, the impact of the implant scan body geometry bevel feature position in relation to the orientation in the patient's mouth on the scan accuracy remains uncertain.

The purpose of the present study was to evaluate the influence of the implant scan body geometry bevel feature location (facial, mesial, distal, lingual, or random), implant angulation (parallel or up to 30°) and implant position in the dental arch on the accuracy (trueness and precision) of complete-arch intraoral digital scans. The null hypotheses were that the implant angulation would have no effect on the trueness and precision of the IOS tested, that the implant angulation would have no effect on the trueness and precision of the IOS tested, that the implant scan body geometry bevel feature position would have no effect on the trueness and precision of the IOS tested, and that the implant position in the dental arch would have no effect on the trueness and precision of the IOS tested.

2. Material and methods

2.1. Reference casts fabrication

A computer-aided design (CAD) software program (Dental Systems 2021, Model Builder; 3Shape A/S) was used to design 2 definitive implant casts (P and NP groups). For the P group, an edentulous maxillary cast was obtained. Four implant abutment analogs (Avinent Transepithelial implant analog digital model; Avinent) were virtually placed in the right first molar (implant 1), right canine (implant 2), left canine (implant 3), and left first molar (implant 4) positions. The implant abutment replicas were positioned at the same apico-coronal height, 3 mm subgingival from the gingival margin of the diagnostic waxed teeth, and with a parallel orientation. For the NP group, the same edentulous maxillary cast, implant abutment analogs, and implant abutment analogs positions and heights were used; however, the implant abutment replicas were virtually placed with up to 30° of angulation among them.

In both virtual definitive implant casts, the implant analog housings were shortened from the intaglio surface to facilitate the posterior engagement between the implant abutment analogs and dental stone. When the definitive implant cast designs were completed, the standard tessellation language (STL) files were exported.

The STL files were used to additively manufacture the polymeric (Nexdent Model 2.0 & Nexdent Gingiva Mask; 3D Systems) casts by using a printer (Nexdent 5100; 3D Systems) following the recommendations of the manufacturer. Then, implant abutment analogs (Avinent Transepithelial implant analog digital model; Avinent) were positioned on each corresponding housing of each implant cast. Subsequently, the base of the casts was filled with Type IV dental stone (GC Fujirock EP; GC) after mixing 22 ml water with 100 g dental stone under vacuum for 30 s per manufacturer's recommendations. The casts were stored at room temperature for 48 h [40]. All the data collection procedures were performed within the 2 following weeks.

Both definitive implant casts (N and NP groups) were digitized by using 2 digitizing methods: a laboratory scanner (7Series Desktop Scanner; Dentalwings) and an IOS (TRIOS 3, Pod, v. 1.7.19.0; 3Shape A/S). The laboratory scan of each definitive implant cast (reference or control) will be used to measure the implant abutment analogs' position discrepancy with the different intraoral digital scans obtained. The manufacturer of the laboratory scanner selected reports an accuracy of 15 μm.

For obtaining the laboratory scan (reference model) of both definitive implant casts, a new implant abutment scan body was positioned on each implant abutment analog (Avinent Transepithelial 4.8 scanbody; Avinent). The implant abutment scan bodies were torqued at 15 Ncm (Torque wrench; Avinent) following the instructions of the manufacturer. The manufacturer's protocol was used to calibrate the extraoral scanner. From each laboratory scan, a STL file was obtained.

2.2. Acquisition of the experimental intraoral digital scans

For obtaining the intraoral digital scans, a room with no windows was selected. The room presented a constant temperature of 24 °C with a 56% relatively humidity. The intraoral scans started and finished on the implant 1 following the scanning pattern recommended by the manufacturer was followed under 1003-lux ambient light illuminance conditions (Fig. 1) [8–10]. The IOS system was color and 3D calibrated before the first scan and after every 10 intraoral digital scans [41]. The scanning pattern was performed following a zigzag technique [42–44]. As reported in previous studies, this scanning pattern started in the right quadrant of the cast from the buccal to palatal and back, slowly and constantly moving forward to the left quadrant of the cast, so that the complete implant scan bodies and gingiva were scanned [42–44].

The intraoral digital scans were obtained by a restorative dentist with 6 years of prior experience handling IOSs (M.G-P). Five subgroups were created based on the position of the anti-rotational flat surface feature of the implant scan bodies: facial (F subgroup), mesial (M subgroup), distal (D subgroup), lingual (L subgroup), or random (R subgroup) surface orientation.

For the P-F and NP-F subgroups, a new implant scan body (Avinent Transepithelial 4.8 scanbody; Avinent) was positioned on each implant abutment analog of both definitive implant casts. The implant scan bodies were positioned with the geometry bevel feature oriented to the facial surface. The implant scan bodies were torqued at 15 Ncm (Torque wrench; Avinent) following the instructions of the manufacturer. The implant scan bodies were maintained until all the digitizing procedures of the P-F and NP-F subgroups were completed. A total of 15 consecutive intraoral digital scans were obtained and exported in a STL file format using the IOS software program. Sample size was determined based on previous studies [45–48].

For the remaining subgroups, the same procedures were replicated as for the P-F and NP-F subgroups, except the geometry bevel feature orientation which varied depending on the subgroup. For the P-M and NP-M subgroups, the geometry bevel feature was orientated towards the mesial surface, for the P-D and NP-D subgroups, the geometry bevel feature of the implant scan bodies was orientated towards the distal surface; for the P-L and NP-L subgroups, the geometry bevel feature of the implant scan bodies was orientated towards the lingual surface; and for the P-R and NP-R subgroups, the geometry bevel feature of the implant scan bodies was orientated randomly towards the facial, mesial, distal, or lingual surfaces. The random position of the implant scan body geometry bevel feature per each implant was determined by using a randomization software program (Random app v1.3; ConnStruct Studios Pty Ltd).

2.3. Measurements

The implant abutment analog position discrepancies between the reference virtual definitive implant casts and their corresponding intraoral digital scans were measured by computing 6 linear inter-implant abutment analog distances and 3 angular measurements among the 4 implant abutment analogs (Fig. 2).

Each STL file obtained on the different experimental intraoral digital

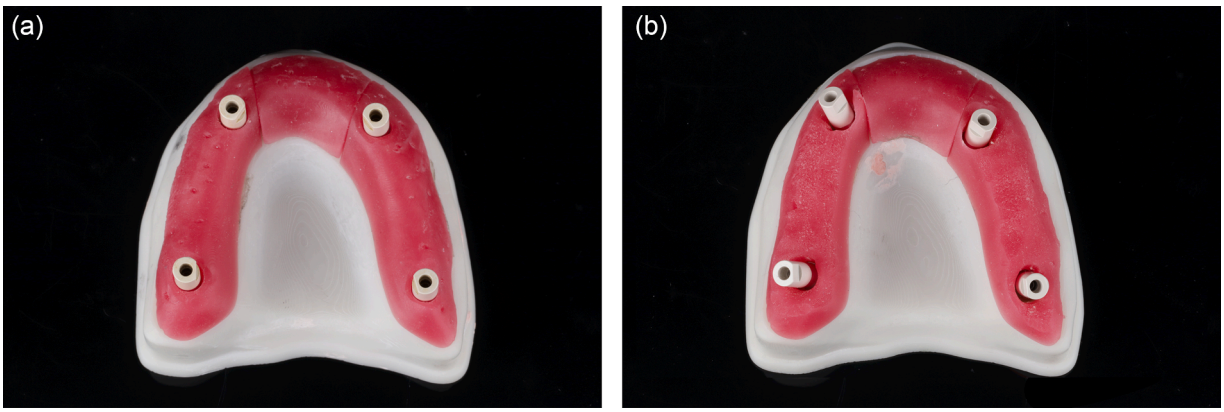

Fig. 1. A, Maxillary definitive implant cast with 4 parallel implant analogs (P group) with the lingual orientation of the geometry bevel feature of the implant scan bodies. B, Maxillary definitive implant cast with 4 non-parallel implant analogs (NP group) with the lingual orientation of the geometry bevel feature of the implant scan bodies.

scans (P-F, P-M, P-D, P-L, P-R, NP-F, NP-M, NP-D, NP-L, and NP-R subgroups) were imported into the CAD software program (Exocad v 2.2 Valetta; Align Technology). The CAD tools were used to align each implant scan body with the corresponding implant scan body from the library of the CAD software program. Subsequently, an implant-supported Ackerman bar design was completed using the CAD tools (Fig. 3). Then, the bar design was exported in an STL file format. Each digital bar design was imported into a CAD software program (Netfabb, v. 2021; Autodesk) to compute the same linear and angular measurements among the different implants. The linear and angular distances computed on each reference virtual definitive implant cast (reference or control) were used to calculate the discrepancies with the linear and angular distances obtained on each experimental intraoral digital scan.

Trueness was defined as the closeness of agreement between a test result and an accepted reference value, or in another words, the average linear measurement discrepancies between the reference and scanned models [40,41]. Precision was described as closeness of agreement between independent results of measurement obtained under stipulated conditions, or as the linear measurement variations per each group or standard deviation (SD) [49,50].

2.4. Statistical analysis

The variable analyzed were implant scan body geometry bevel feature position, implant angulation, and implant position in the dental arch. The Shapiro-Wilk and Kolmogorov-Smirnov tests revealed that the data were normally distributed ($P > .05$). Both outcome variables including linear and angular measurements were transformed using square root method after which the residuals were normally distributed, and no patterns were visible on residuals versus fits plot. Three-way ANOVA followed by the pairwise comparison Tukey tests were used to analyze the data using a statistical software program (IBM SPSS Statistics for Windows, v26; IBM Corp) ($\alpha = .05$).

3. Results

Three-way ANOVA analysis of variance showed that the geometry bevel feature position ($df = 1$, $MS = 0.1342$, $F = 7.92$, $P < .001$) and the inter-implant distance measurement ($df = 5$, $MS = 0.7154$, $F = 42.25$, $P < .001$) were significant predictors of the linear discrepancies obtained; however, 3-way ANOVA analysis of variance showed that the group (P or NP groups) variable was not a significant predictor ($df = 1$, $MS =$

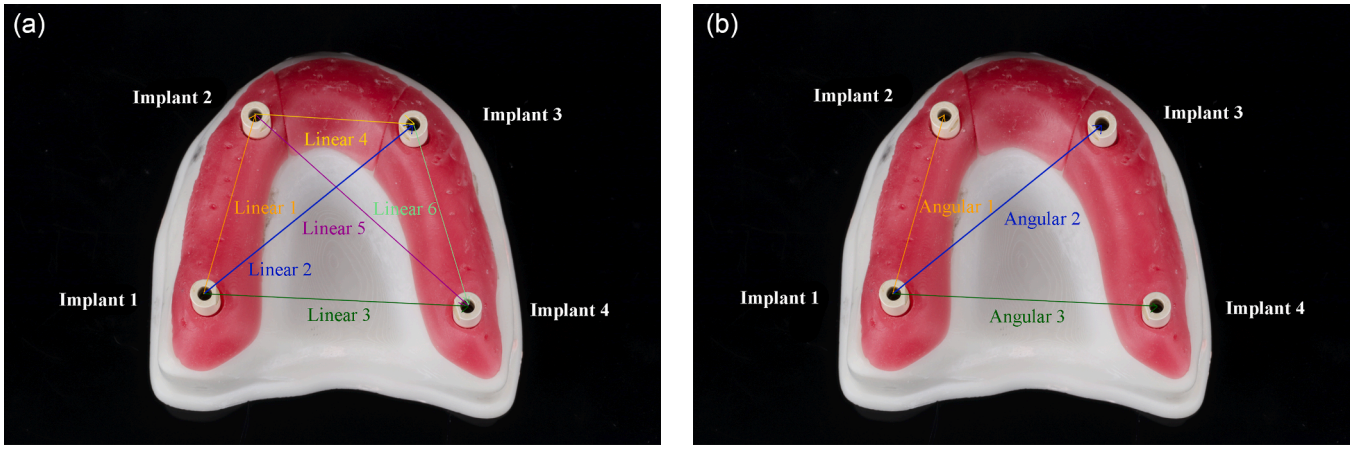

Fig. 2. A, Representative linear measurements among the 4 implant abutment analogs on each reference virtual definitive cast and experimental intraoral digital scans. B, Representative angular measurements among the 4 implant abutment analogs on each reference virtual definitive cast and experimental intraoral digital scans.

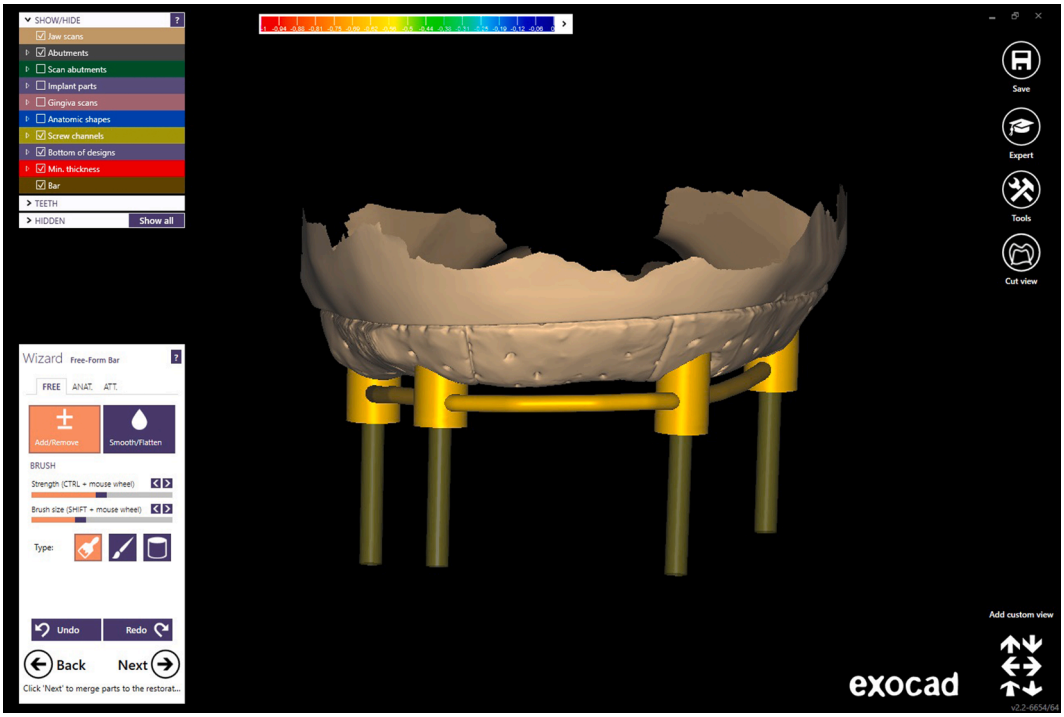

Fig. 3. Representative digital implant-supported Ackerman bar design.

0.0071, F = 0.42, P = .517) on the linear discrepancies calculated (Fig. 4AB). Furthermore, the geometry bevel feature position explains the 2.80% of variation in the linear discrepancies computed, while the inter-implant distance measurement explains the 18.65% of variation in the measurement discrepancies found (Table 1).

Tukey pairwise comparison showed that only the linear measurement of L subgroup (0.29) was significantly lower from the rest of the subgroups (Table 2) (Fig. 4C). Also, Tukey pairwise comparison showed that there were significant differences among the different inter-implant distances tested (Table 3) (Fig. 4D).

Three-way ANOVA analysis of variance showed that the implant angulation (df = 1, MS = 8.6506, F = 162.83, P < .001), the geometry bevel feature position (df = 4, MS = 0.5841, F = 11.00, P < .001), and the inter-implant distance measurement (df = 2, MS = 6.0111, F = 113.15, P < .001) were all significant predictors of the angular measurement discrepancies obtained. Additionally, the implant angulation feature position explains the 18.61%, the geometry bevel feature position the 5.03%, and the inter-implant angulation measurement the 25.85% of variation in the angular measurement discrepancies computed (Fig. 5AB).

Tukey pairwise comparison showed a significant mean angular measurement difference between them with a mean of 0.92 for angulated and 0.64 for parallel (Fig. 5C). Tukey pairwise comparison demonstrated significant differences among the different geometry bevel positions tested. Tukey pairwise comparison showed significant differences between the angular measurements of L and B, M and B, R and B, M and D, and R and D (Table 4) (Fig. 5D).

4. Discussion

Based on the results of the present study, the lingual orientation of the implant scan body geometry bevel feature computed the highest trueness and precision values when compared with the remaining orientations tested. Additionally, the implant abutment analog position on the definitive implant cast, as well as the implant abutment analog angulation were identified as significant predictors for the trueness and precision mean values obtained. Therefore, all the null hypotheses were rejected.

In the best knowledge of the authors, this is the first investigation that assessed the influence of the implant scan body geometry bevel feature position on the complete-arch intraoral scanning accuracy. The results of this study revealed that the location of the geometry bevel feature of the scan body can decrease the scanning accuracy of the IOS system tested. In this investigation, the lingual orientation demonstrated the lowest linear and angular measurement discrepancies or the highest accuracy values compared with the rest of the orientations tested. However, additional clinical studies are needed to assess the influence of this parameter on intraoral implant scanning accuracy.

Previous literature has evaluated the influence of implant angulation on the accuracy of IOSs; however, contradictory results have been reported [28–32]. A systematic review and meta-analysis, based mostly on *in-vitro* studies, compared conventional and intraoral digital scans in completely and partially edentulous scenarios [31]. The authors concluded that the implant angulation decreased the accuracy of the digital scans when compared to the conventional impression techniques; however, the difference was not statistically significant [31]. Similarly, an *in-vitro* study compared conventional and intraoral digital scans using a partially edentulous mandibular cast with 4 implant analogs [29]. The right quadrant of the mandibular reference cast had the 2 implant analogs parallel, but on the left side the implant analogs were placed with 20° convergence. Results showed that the implant angulation did not influence the overall definitive implant cast accuracy [29]. Comparisons with the present study are difficult due to differing number, position, type, and angulation of the implant abutment analogs, digitizing procedures, and measurement methods. Furthermore, the implant scan body anti-rotational feature orientation was not described.

On the other hand, a study by Lin et al. [32] compared conventional and intraoral digital scans of 4 casts with 2 implant analogs placed parallel and at 3 different angles (15, 30, and 45°). Authors reported that the intraoral digital scans of the implant analogs having 0- and 15° divergence showed lower accuracy compared with the conventional methods. Additionally, the intraoral digital scans of 30° implant divergence revealed no difference in angular measurements when compared to the conventional group. At 45° implant divergence both angular and

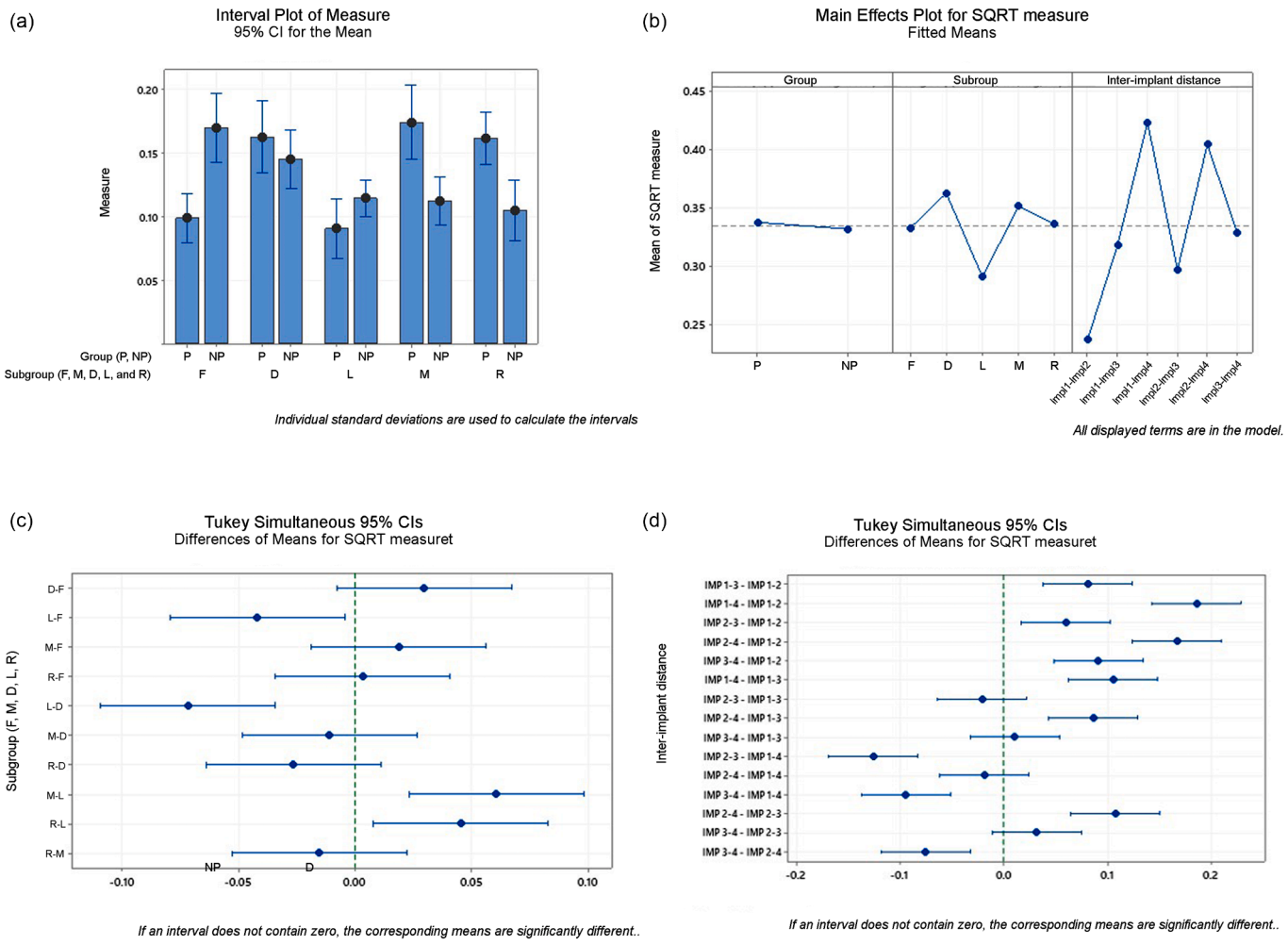

Fig. 4. Linear measurement analysis. A, Interval plot. B, Main effects plot. C, Tukey for pairwise comparisons grouping the data by the anti-rotational feature position. D, Tukey for pairwise comparisons grouping the data by inter-implant distance measured. D, distal; F, facial; M, mesial; NP, non-parallel; L, lingual; P, parallel; R, random.

Table 1
Descriptive statistics of the overall linear and angular measurement discrepancies computed on the different groups tested.

Group	Subgroup	Overall linear measurement discrepancies mean ±standard deviation (trueness ±precision) (mm)	Overall angular measurement discrepancies mean ±standard deviation (trueness ±precision) (degrees)
P	F	0.099 ±0.091	0.391 ± 0.200
	M	0.174 ±0.138	0.611 ± 0.424
	D	0.162 ±0.136	0.401 ± 0.350
	L	0.090 ±0.112	0.503 ± 0.251
	R	0.161 ±0.097	0.472 ± 0.361
NP	F	0.170 ±0.129	0.621 ± 0.416
	M	0.112 ±0.090	0.993 ± 0.414
	D	0.145 ±0.110	0.861 ± 0.396
	L	0.114 ±0.070	0.863 ± 0.585
	R	0.105 ±0.115	1.369 ± 0.759

D, distal; F, facial; L, lingual; M, mesial; NP, non-parallel; P, parallel, R, random

distance measurements were comparable to the conventional group. The results suggested that the digital scans showed better results when the inter-implant angulation was greater than 30° [32]. Arcuri et al. [28] reported that the implant angulation could negatively affect the accuracy of the intraoral complete-arch digital scans. Comparisons with the present study are challenging due to differing research protocols.

Table 2
Tukey pairwise comparisons grouping the information by the geometry bevel feature position (F, M, D, L, A) using the Tukey method and 95% confidence interval. D, distal; F, facial; M, mesial; L, lingual; R, random.

Subgroup	Mean overall linear measurement discrepancy
F	0.362[a]
M	0.351[a]
D	0.336[a]
L	0.333[a]
R	0.291[b]

Means that do not share a letter are significantly different ($P < .05$)

Table 3
Tukey pairwise comparisons grouping the information by the inter-implant distance tested using the Tukey method and 95% confidence interval.

Inter-implant distance	Mean overall linear measurement discrepancy
Linear-3	0.423[a]
Linear-5	0.404[a]
Linear-6	0.328[b]
Linear-2	0.318[b]
Linear-4	0.297[b]
Linear-1	0.237[c]

Means that do not share a letter are significantly different ($P < .05$).

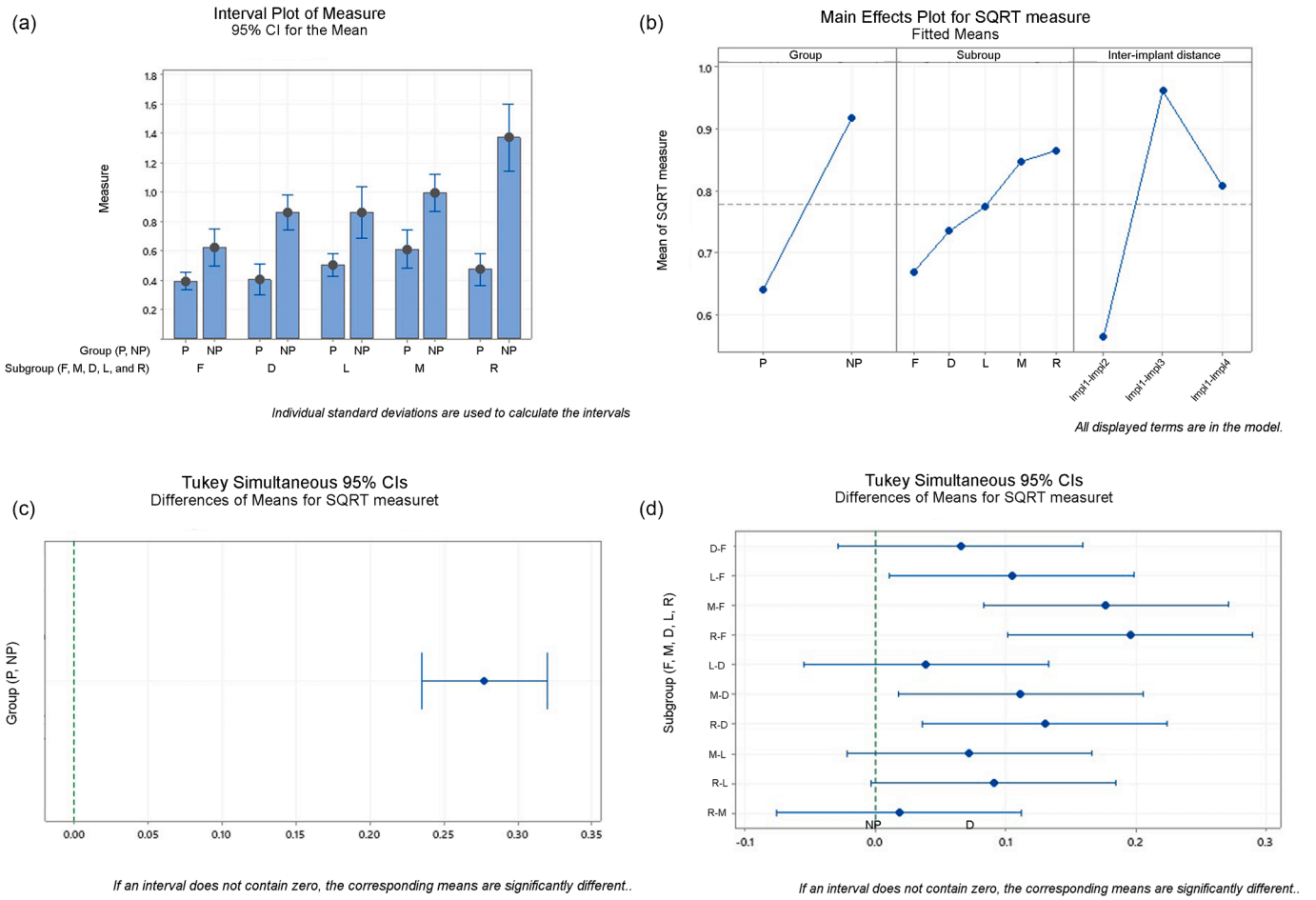

Fig. 5. Angular measurement analysis. A, Interval plot. B, Main effects plot. C, Tukey for pairwise comparisons grouping the data by the P and NP groups. D, Tukey for pairwise comparisons grouping the data by the anti-rotational feature position tested. A, arbitrary; D, distal; F, facial; M, mesial; L, lingual.

Table 4
Tukey pairwise comparisons grouping the information by the inter-implant distance tested using the Tukey method and 95% confidence interval. D, distal; F, facial; M, mesial; L, lingual; R, random.

Geometry bevel feature position	Mean overall angular measurement discrepancy
F	0.669[c]
M	0.846[a]
D	0.735[b,c]
L	0.774[a,b]
R	0.865[a]

Means that do not share a letter are significantly different ($P < .05$).

Additionally, the implant scan body geometry bevel feature orientation was not disclosed.

The influence of the implant position in the dental arch on the intraoral scanning accuracy has not been assessed previously, as dental literature usually reports the overall implant position discrepancy. Based on the results of the present study, the linear measurements 3 and 5 obtained the highest discrepancy values, while the linear measurement obtained the lowest discrepancy values. A pattern can be observed in which the implant where the intraoral digital scan is finished (implant positioned in the left first molar) presented higher discrepancy than the contralateral implant (implant positioned in the right first molar). This could be explained by the accumulative distortion during the stitching procedures in the data acquisition process. However, further studies are needed to comprehend this outcome. Additionally, previous studies have reported that the higher the inter-implant distance, the higher the intraoral scanning deviations obtained [35–37]. In the present study, the implant analogs might not represent the ideal position aiming to increase the inter-implant distance.

In the present investigation, the scanning conditions, including scanning pattern [6,7] and ambient light illuminance conditions [8–10], were standardized to minimize the variables that can affect IOSs accuracy. The implant scan body selected was fabricated in polyetheretherketone (PEEK) material, which might have influenced the results obtained; however, all the intraoral digital scans were acquired using the same implant scan body and new implant scan bodies were used. Therefore, the results obtained can be compared among the different subgroups tested. Additionally, the present study presents several limitations such as the laboratory conditions, the single scan body geometry and material tested, and testing with only one IOS.

Additional studies are recommended to further evaluate the influence of the scan body material, geometry, geometry bevel orientation, implant position, implant type, or extension of the implant digital scan on the intraoral scanning accuracy of IOSs. Dental literature might require additional data before systematic clinical recommendations can be formulated. Additionally, hardware and software advancements are continuous and progressive, and therefore, data obtained from older systems should be considered carefully. An understanding of this literature limitation is fundamental for the evidence-based implementation of digital technologies in the dental field.

5. Conclusions

Within the limitations of this *in-vitro* study, the following conclusions were drawn:

- The implant scan body geometry bevel feature location, implant angulation and implant position in the dental arch influenced the accuracy (trueness and precision) of the IOS tested.
- The lingual orientation of the implant scan body geometry bevel feature obtained significantly higher trueness and precision values compared with the facial, mesial, distal, or random positions tested.
- Implant angulation decreased intraoral scanning accuracy (trueness and precision) of the IOS tested.
- The implant positioned in the dental arch where the intraoral digital scan is finished obtained significantly higher distortion than the contralateral implant.

CRediT authorship contribution statement

Miguel Gómez-Polo: Supervision, Conceptualization, Methodology, Visualization, Writing – original draft. **Francisco Álvarez:** Data curation, Methodology. **Rocío Ortega:** Data curation, Methodology. **Cristina Gómez-Polo:** Conceptualization, Methodology. **Abdul B. Barmak:** Formal analysis, Visualization, Writing – original draft. **John C. Kois:** Visualization, Writing – review & editing. **Marta Revilla-León:** Methodology, Formal analysis, Visualization, Writing – original draft.

Declaration of Competing Interest

The authors declare that they have no known competing financial interests or personal relationships that could have appeared to influence the work reported in this paper.

Funding

This research did not receive any specific grant from funding agencies in the public, commercial, or not-for-profit sectors.

References

[1] K.M. Chochlidakis, P. Papaspyridakos, A. Geminiani, C.J. Chen, I.J. Feng, C. Ercoli, Digital versus conventional impressions for fixed prosthodontics: a systematic review and meta-analysis, J. Prosthet. Dent. 116 (2016) 184–190, https://doi.org/10.1016/j.prosdent.2015.12.017.

[2] M. Tabesh, F. Nejatidanesh, G. Savabi, A. Davoudi, O. Savabi, H. Mirmohammadi, Marginal adaptation of zirconia complete-coverage fixed dental restorations made from digital scans or conventional impressions: a systematic review and meta-analysis, J. Prosthet. Dent. 125 (2021) 603–610, https://doi.org/10.1016/j.prosdent.2020.01.035.

[3] L. Giachetti, C. Sarti, F. Cinelli, D.S. Russo, Accuracy of digital impressions in fixed prosthodontics: a systematic review of clinical studies, Int. J. Prosthodont. 33 (2020) 192–201, https://doi.org/10.11607/ijp.6468.

[4] K. Chochlidakis, P. Papaspyridakos, A. Tsigarida, D. Romeo, Y.W. Chen, Z. Natto, C. Ercoli, Digital versus conventional full-arch implant impressions: a prospective study on 16 edentulous maxillae, J. Prosthodont. 29 (2020) 281–286, https://doi.org/10.1111/jopr.13162.

[5] F. Kernen, S. Schlager, V. Seidel Alvarez, J. Mehrhof, K. Vach, R. Kohal, K. Nelson, T. Flügge, Accuracy of intraoral scans: an *in vivo* study of different scanning devices, J. Prosthet. Dent. (2021), https://doi.org/10.1016/j.prosdent.2021.03.007.

[6] K.C. Oh, J.M. Park, H.S. Moon, Effects of scanning strategy and scanner type on the accuracy of intraoral scans: a new approach for assessing the accuracy of scanned data, J. Prosthodont. 29 (2020) 518–523, https://doi.org/10.1111/jopr.13158.

[7] P. Müller, A. Ender, T. Joda, J. Katsoulis, Impact of digital intraoral scan strategies on the impression accuracy using the TRIOS Pod scanner, Quintessence. Int. 47 (2016) 343–349, https://doi.org/10.3290/j.qi.a35524.

[8] M. Revilla-León, P. Jiang, M. Sadeghpour, W. Piedra-Cascón, A. Zandinejad, M. Özcan, V.R. Krishnamurthy, Intraoral digital scans-part 1: influence of ambient scanning light conditions on the accuracy (trueness and precision) of different intraoral scanners, J. Prosthet. Dent. 124 (2020) 372–378, https://doi.org/10.1016/j.prosdent.2019.06.003.

[9] M. Revilla-León, S.G. Subramanian, M. Özcan, V.R. Krishnamurthy, Clinical study of the influence of ambient light scanning conditions on the accuracy (trueness and precision) of an intraoral scanner, J. Prosthodont. 29 (2020) 107–113, https://doi.org/10.1111/jopr.13135.

[10] M. Revilla-León, S.G. Subramanian, W. Att, V.R. Krishnamurthy, Analysis of different illuminance of the room lighting condition on the accuracy (trueness and precision) of an intraoral scanner, J. Prosthodont. 30 (2021) 157–162.

[11] P. Medina-Sotomayor, A. Pascual-Moscardó, I. Camps, Relationship between resolution and accuracy of four intraoral scanners in complete-arch impressions, J. Clin. Exp. Dent. 10 (2018) 361–366, https://doi.org/10.1111/jopr.13276.

[12] T. Joda, F. Zarone, M. Ferrari, The complete digital workflow in fixed prosthodontics: a systematic review, BMC Oral Health 17 (2017) 124, https://doi.org/10.1186/s12903-017-0415-0.

[13] W. Renne, M. Ludlow, J. Fryml, Z. Schurch, A. Mennito, R. Kessler, A. Lauer, Evaluation of the accuracy of 7 digital scanners: an *in vitro* analysis based on 3-dimensional comparisons, J. Prosthet. Dent. 118 (2017) 36–42, https://doi.org/10.1016/j.prosdent.2016.09.024.

[14] H. Hayama, K. Fueki, J. Wadachi, N. Wakabayashi, Trueness and precision of digital impressions obtained using an intraoral scanner with different head size in the partially edentulous mandible, J. Prosthodont. Res. 62 (2018) 347–352, https://doi.org/10.1016/j.jpor.2018.01.003.

[15] Y.G. Moon, K.M. Lee, Comparison of the accuracy of intraoral scans between complete-arch scan and quadrant scan, Prog. Orthod. 21 (2020) 36, https://doi.org/10.1186/s40510-020-00337-1.

[16] M.K. Kim, K. Son, B.Y. Yu, K.B. Lee, Effect of the volumetric dimensions of a complete arch on the accuracy of scanners, J. Adv. Prosthodont. 12 (2020) 361–368, https://doi.org/10.4047/jap.2020.12.6.361.

[17] M. Waldecker, S. Rues, C. Trebing, R. Behnisch, P. Rammelsberg, W. Bömicke, Effects of training on the execution of complete-arch scans. Part 2: scanning accuracy, Int. J. Prosthodont. 34 (2021) 27–36, https://doi.org/10.4047/jap.2020.12.6.361.

[18] J.H. Lim, J.M. Park, M. Kim, S.J. Heo, J.Y. Myung, Comparison of digital intraoral scanner reproducibility and image trueness considering repetitive experience, J. Prosthet. Dent. 119 (2018) 225–232, https://doi.org/10.1016/j.prosdent.2017.05.002.

[19] J. Kim, J.M. Park, M. Kim, S.J. Heo, I.H. Shin, M. Kim, Comparison of experience curves between two 3-dimensional intraoral scanners, J. Prosthet. Dent. 116 (2016) 221–230, https://doi.org/10.1016/j.prosdent.2015.12.018.

[20] S.H. Shin, H.S. Yu, J.Y. Cha, J.S. Kwon, C.J. Hwang, Scanning accuracy of bracket features and slot base angle in different bracket materials by four intraoral scanners: an *in vitro* study, Materials 14 (2021) 365, https://doi.org/10.3390/ma14020365 (Basel).

[21] R. Jin-Young Kim, G.I. Benic, J.M. Park, Trueness of intraoral scanners in digitizing specific locations at the margin and intaglio surfaces of intracoronal preparations, J. Prosthet. Dent. 126 (2021) 779–786, https://doi.org/10.1016/j.prosdent.2020.09.019.

[22] J.W. Anh, J.M. Park, Y.S. Chun, M. Kim, M. Kim, A comparison of the precision of three-dimensional images acquired by 2 digital intraoral scanners: effects of tooth irregularity and scanning direction, Korean J. Orthod. 46 (2016) 3–12, https://doi.org/10.4041/kjod.2016.46.1.3.

[23] H. Li, P. Lyu, Y. Wang, Y. Sun, Influence of object translucency on the scanning accuracy of a powder-free intraoral scanner: a laboratory study, J. Prosthet. Dent. 117 (2017) 93–101, https://doi.org/10.1016/j.prosdent.2016.04.008.

[24] R.M. Mizumoto, B. Yilmaz, E.A. McGlumphy, J. Seidt, W.M. Johnston, Accuracy of different digital scanning techniques and scan bodies for complete-arch implant-supported prostheses, J. Prosthet. Dent. 123 (2020) 96–104, https://doi.org/10.1016/j.prosdent.2019.01.003.

[25] Z. Nagy, B. Simon, A. Mennito, Z. Evans, W. Renne, J. Vág, Comparing the trueness of seven intraoral scanners and a physical impression on dentate human maxilla by a novel method, BMC Oral Health 20 (2020) 97, https://doi.org/10.1186/s12903-020-01090-x.

[26] R.M. Mizumoto, B. Yilmaz, Intraoral scan bodies in implant dentistry: a systematic review, J. Prosthet. Dent. 120 (2018) 343–352, https://doi.org/10.1016/j.prosdent.2017.10.029.

[27] T. Fluegge, W. Att, M. Metzger, K. Nelson, A novel method to evaluate precision of optical implant impressions with commercial scan bodies-an experimental approach, J. Prosthodont. (26) (2017) 34–41, https://doi.org/10.1111/jopr.12362.

[28] M. Moslemion, L. Payaminia, H. Jalali, M. Alikhasi, Do type and shape of scan bodies affect accuracy and time of digital implant impressions? Eur. J. Prosthodont. Restor. Dent. 28 (2020) 18–27, https://doi.org/10.1922/EJPRD_1962Moslemion10.

[29] L. Arcuri, A. Pozzi, F. Lio, E. Rompen, W. Zechner, A. Nardi, Influence of implant scanbody material, position and operator on the accuracy of digital impression for complete-arch: a randomized *in vitro* trial, J. Prosthodont. Res. 64 (2020) 128–136, https://doi.org/10.1016/j.jpor.2019.06.001.

[30] K. Basaki, H. Alkumru, G. De Souza, Y. Finer, Accuracy of digital vs conventional implant impression approach: a three-dimensional comparative *in vitro* analysis, Int. J. Oral Maxillofac. Implants 32 (2017) 792–799, https://doi.org/10.11607/jomi.5431.

[31] A.L. Carneiro Pereira, V.R. Medeiros, A. da Fonte Porto Carreiro, Influence of implant position on the accuracy of intraoral scanning in fully edentulous arches: a systematic review, J. Prosthet. Dent. 126 (2021) 749–755, https://doi.org/10.1016/j.prosdent.2020.09.008.

[32] P. Papaspyridakos, K. Vazouras, Y.W. Chen, E. Kotina, Z. Natto, K. Kang, K Chochlidakis, Digital vs conventional implant impressions: a systematic review and meta-analysis, J. Prosthodont. 29 (2020) 660–678, https://doi.org/10.1111/jopr.13211.

[33] W.S. Lin, B.T. Harris, E.N. Elathamna, T. Abdel-Azim, D. Morton, Effect of implant divergence on the accuracy of definitive casts created from traditional and digital implant-level impressions: an *in vitro* comparative study, Int. J. Oral Maxillofac. Implants 30 (2015) 102–109, https://doi.org/10.11607/jomi.3592.
[34] B. Giménez-González, B. Hassan, M. Özcan, G. Pradíes, An *in vitro* study of factors influencing the performance of digital intraoral impressions operating on active wavefront sampling technology with multiple implants in the edentulous maxilla, J. Prosthodont. 26 (2017) 650–655, https://doi.org/10.1111/jopr.12457.
[35] B. Giménez, M. Ozcan, F. Martínez-Rus, G. Pradíes, Accuracy of a digital impression system based on active triangulation technology with blue light for implants: effect of clinically relevant parameters, Implant Dent. 24 (2015) 498–504, https://doi.org/10.1097/ID.0000000000000283.
[36] Y.J. Zhang, J.Y. Shi, S.J. Qian, S.C. Qiao, H.C. Lai, Accuracy of full-arch digital implant impressions taken using intraoral scanners and related variables: a systematic review, Int. J. Oral Implantol. 14 (2021) 157–179 (Berl.).
[37] Y.D. Choi, K.E. Lee, H.N. Mai, D.H. Lee, Effects of scan body exposure and operator on the accuracy of image matching of implant impressions with scan bodies, J. Prosthet. Dent. 124 (2020) 379.e1, https://doi.org/10.1016/j.prosdent.2020.04.004. -6.
[38] R. Richert, A. Goujat, L. Venet, G. Viguie, S. Viennot, P. Robinson, J.C. Farges, M. Fages, M. Ducret, Intraoral scanners technologies: a review to make a successful impression, J. Healthc. Eng. 2017 (2017), 8427595, https://doi.org/10.1155/2017/8427595.
[39] U. Lawitschka, F. Homann, B. Straub. Determining position and orientation of a dental implant. European Patent - EP2218423A1. 2010.
[40] E.R. Schwedhelm, X. Lepe, Fracture strength of type IV and type V die stone as a function of time, J. Prosthet. Dent. 78 (1997) 554–559, https://doi.org/10.1016/s0022-3913(97)70005-2.
[41] M. Revilla-León, A. Gohil, A.B. Barmak, M. Gómez-Polo, J.A. Pérez-Barquero, W. Att, J.C. Kois, Influence of ambient temperature changes on intraoral scanning accuracy, J. Prosthet. Dent. (2022), https://doi.org/10.1016/j.prosdent.2022.01.012.
[42] R.J. Kim, J.M. Park, J.S. Shim, Accuracy of 9 intraoral scanners for complete-arch image acquisition: a qualitative and quantitative evaluation, J. Prosthet. Dent. 120 (2018) 895–903, https://doi.org/10.1016/j.prosdent.2018.01.035.
[43] P. Medina-Sotomayor, M.A. Pascual, A.I. Camps, Accuracy of four digital scanners according to scanning strategy in complete-arch impressions, PLoS One 13 (2018), e0202916, https://doi.org/10.1371/journal.pone.0202916.
[44] F.G. Mangano, U. Hauschild, G. Veronesi, M. Imburgia, C. Mangano, O. Admakin, Trueness and precision of 5 intraoral scanners in the impressions of single and multiple implants: a comparative *in vitro* study, BMC Oral Health 19 (2019) 101, https://doi.org/10.1186/s12903-019-0792-7.
[45] A. Ender, M. Zimmermann, A. Mehl, Accuracy of complete- and partial-arch impressions of actual intraoral scanning systems *in vitro*, Int. J. Comput. Dent. 22 (2019) 11–19. PMID: 30848250.
[46] A. Sallorenzo, M. Gómez-Polo, Comparative study of the accuracy of an implant intraoral scanner and that of a conventional intraoral scanner for complete-arch fixed dental prostheses, J. Prosthet. Dent. (2021), https://doi.org/10.1016/j.prosdent.2021.01.032. Epub ahead of print.
[47] H. Gao, X. Liu, M. Liu, X. Yang, J. Tan, Accuracy of three digital scanning methods for complete-arch tooth preparation: an *in vitro* comparison, J. Prosthet. Dent. (2021), https://doi.org/10.1016/j.prosdent.2021.01.029. Epub ahead of print.
[48] J.C. Treesh, P.C. Liacouras, R.M. Taft, D.I. Brooks, S. Raiciulescu, D.O. Ellert, G. T. Grant, L. Ye, Complete-arch accuracy of intraoral scanners, J. Prosthet. Dent. 120 (2018) 382–388, https://doi.org/10.1016/j.prosdent.2018.01.005.
[49] International Organization for Standardization. ISO 5725-1:1994. Accuracy (trueness and precision) of measurement methods and results - part 1: general principles and definitions. https://www.iso.org/obp/ui/#iso:std:iso:5725:-1:ed-1:v1:en Accessed 02-01-20.
[50] International Organization for Standardization. ISO 20896-1:2019. Dentistry-digital impression devices-part 1: methods for assessing accuracy. https://www.iso.org/standard/69402.html Accessed 02-01-20.